UDK 621.785.54:691.714
Original scientific article/Izvirni znanstveni članek

ISSN 1580-2949
MTAEC9, 58(5)647(2024)

EFFECT OF Nb, Ta, AND Ti MICROALLOYING ON THE SECONDARY HARDENING OF Mo-W TOOL STEEL

VPLIV MIKROLEGIRANJA Nb, Ta IN Ti NA SEKUNDARNO UTRJEVANJE Mo-W ORODNEGA JEKLA

Jaka Burja[1,2*], Aleš Nagode[2], Klemen Grabnar[2,3], Jožef Medved[2], Tilen Balaško[2]

[1]Institute of Metals and Technology, Lepi pot 11, 1000 Ljubljana, Slovenia
[2]Faculty of Natural Sciences and Engineering, University of Ljubljana, Aškerčeva cesta 12, 1000 Ljubljana, Slovenia
[3]Metal Tech Solutions d.o.o., Trubarjeva ulica 91, 3000 Celje, Slovenia

Prejem rokopisa – received: 2024-06-04; sprejem za objavo – accepted for publication: 2024-09-04

doi:10.17222/mit.2024.1210

This work investigates the influence of microalloying elements on the tempering process of a hot-work tool steel. The study examines the austenitisation temperatures and grain growth of a high thermal conductivity hot-work tool steel, with the addition of various microalloying elements: Nb+0.06 *w*/% Nb, Ta+0.03 *w*/% Ta, and Ti+0.006 *w*/% Ti, compared to a reference sample. Thermodynamic calculations are used to analyse the influence of microalloying on the transformation temperatures and carbide formation. Austenitisation temperatures of (1030, 1060, 1080, and 1100) °C are selected, and subsequent tempering is performed at (540, 580, 600, 620, and 640) °C. The investigation focuses on analysing the microstructure, hardness, and grain size. The results show that the microalloying elements have a positive influence on the retention of the grain size during austenitisation and on the enhancement of hardness during tempering. Electron microscopy is utilized to analyse the microstructure, which indicates the prevalence of Mo-W carbides. The carbides exhibit coarsening and morphological changes during high-temperature tempering. The secondary hardening peaks occur at temperatures between (600 and 620) °C, and are more pronounced by microalloying.

Keywords: hot work tool steel, microalloying, tempering, heat treatment, carbides

Raziskovali smo vpliv mikrolegirnih elementov na postopek utrjevanja orodnega jekla za delo v vročem. Analizirali smo vpliv temperature avstenitizacije na rast zrn visoko toplotno prevodnega orodnega jekla ob dodatku različnih mikrolegirnih elementov: Nb+0,06 *w*/% Nb, Ta+0,03 *w*/% Ta in Ti+0,006 *w*/% Ti v primerjavi z referenčnim vzorcem. S termodinamičnimi izračuni smo analizirali vpliv mikrolegiranja na temperature premen in tvorbo karbidov. Izbrane temperature avstenitizacije so bile (1030, 1060, 1080 in 1100) °C, nato smo vzorce popuščali pri (540, 580, 600, 620 in 640) °C. Analizirali smo mikrostrukturo, trdote in velikosti zrn. Rezultati kažejo, da mikrolegirni elementi pozitivno vplivajo na ohranjanje velikosti zrn med avstenitizacijo in na povečanje trdote med popuščanjem. Z elektronsko mikroskopijo smo analizirali mikrostrukture, v kateri prevladujejo Mo-W karbidi. Ti karbidi pri visokih temperaturah popuščanja rastejo in spremenijo obliko. Vrhovi sekundarnega utrjevanja se pojavijo pri temperaturah med 600 °C in 620 °C ter so bolj izraziti pri mikrolegiranju.

Ključne besede: orodno jeklo za delo v vročem, mikrolegiranje, popuščanje, toplotna obdelava, karbidi

1 INTRODUCTION

Hot-work tool steels are high-quality steels valued for their exceptional mechanical properties at elevated temperatures. These properties are essential for their applications in demanding environments of high temperatures and high heat fluxes. The combination of strength, hardness, toughness, wear resistance, thermo-cyclic stability, and thermal conductivity make hot-work tool steels indispensable.[1–6] Widely used in the manufacturing of dies for extrusion, forging, and especially light-metal die casting, these steels are subjected to severe cyclic thermal and mechanical stresses, adhesion, abrasion, and thermal dissolution. Degradation of these steels primarily results from a combination of low-cycle fatigue and thermal fatigue, arising from frequent temperature fluctuations during service.[7,8]

Achieving the desired mechanical properties in hot-work tool steels requires precise control of the steel's chemical composition and the formation of a suitable, stable microstructure through heat treatment. Tempered martensite and alloy-carbide precipitates typically form within the microstructure of these steels.[9–12]

The heat-treatment process for hot-work tool steels involves three stages: austenitisation, quenching, and tempering. Fine, undissolved carbides, nitrides, or carbonitrides play a crucial role in the austenitisation stage by preventing the growth of austenite crystal grains through their pinning effect at grain boundaries.[5,13,14] Small crystal grains are essential for achieving the desired mechanical properties. Conversely, coarse prior-austenite crystal grains negatively impact the steel's strength and impact toughness, especially at low temperatures.[15–17]

To suppress grain growth, microalloying elements (e.g., Nb, Ta, V, Ti) are added to the steel.[5,12,18] Additionally, alloyed carbide precipitates are instrumental in

*Corresponding author's e-mail:
jaka.burja@imt.si (Jaka Burja)

Table 1: Chemical compositions of the experimental charges (*w*/%)

Sample	C	Si	Ni	Mo	W	Nb	Ta	Ti	Fe
0	0.32	0.04	0.03	3.2	1.7	/	/	/	balance
Nb	0.32	0.05	0.03	3.2	1.7	0.06	/	/	balance
Ta	0.32	0.05	0.03	3.2	1.7	/	0.03	/	balance
Ti	0.32	0.04	0.03	3.2	1.7	/	/	0.006	balance

secondary hardening during the tempering process. The type of carbide precipitates formed in hot-work tool steels depends on the steel's chemical composition and the tempering temperatures. Common carbide types found in hot-work tool steels include V-rich (MC), Mo- and/or W-rich (M_6C, M_2C), and Cr-rich (M_3C, M_7C_3, and $M_{23}C_6$) carbides.[4,5] However, at temperatures exceeding the maximum for secondary hardening, alloy carbides gradually coarsen, and the dislocation density decreases. Ultimately, the martensitic matrix transforms into a ferritic structure, leading to a significant softening of the steel.[7]

The relationship between steel softening and carbide coarsening was first described by Hollomon and Jaffe.[19] By delaying carbide coarsening, the deterioration of the martensitic microstructure can be slowed down.[9,12,20,21] This results in the retention of hardness and high-temperature fatigue strength at higher temperatures and for extended durations. Consequently, understanding the microstructure evolution during tempering and service is crucial for optimizing the tool life.[22]

While the effect of microalloying elements (V, Nb, or Ti) on the quenching and tempering processes of low-alloy steels has been extensively studied, their impact on the tempering process of higher alloy steels exhibiting secondary hardening peaks remains less understood.[14,23–25] This is particularly true for Mo-W tool steels with increased thermal conductivity values up to 60 $W \cdot mK^{-1}$, where we have briefly described the effect in previous papers but have paid more attention to the thermodynamics and characterization in the current work.[26–28]

The objective of this study is to further investigate the influence of microalloying elements (Nb, Ta, and Ti) on the tempering process of Mo-W hot-work steel. The role of these microalloying elements in the microstructural evolution and the development of secondary hardening peaks during tempering will be examined.

2 EXPERIMENTAL PART

A total of four steel compositions were melted and cast into a 60 × 60 × 400 mm^3 ingot. The first charge was made as a reference without additional alloying, to better describe the base properties (steel composition 0). The second composition had 0.06 *w*/% Nb added (Nb – **Table 1**), the third composition had 0.03 *w*/% Ta added (Ta – **Table 1**) and the composition had 0.006 *w*/% Ti added (Ti – **Table 1**). The chemical composition (**Table 1**) was measured by wet chemical analysis and infrared absorption after combustion with an ELTRA CS-800.

The ingots were cooled to room temperature in the air after casting. Then they were annealed at 720 °C for 2 h to relieve stress, and soften for further processing. Any possible surface defects were ground off, and the ingot head was cut off to remove the shrinkage porosity. The ingots were then homogenised at 1200 °C for 1 h and hot rolled into billets measuring (40 × 40) mm. After hot rolling, the billets were slowly cooled to room temperature in ceramic wool. The billets were then heated to 1100 °C and hot forged into square bars measuring (18 × 18) mm. The bars were then slowly cooled to room temperature in ceramic wool. After cooling to room temperature, the samples were ground to remove the oxide scale. Then the samples were soft annealed for 1.5 h at 770 °C in a vacuum hardening furnace type Ipsen Turbo XL treater under vacuum.

Then the samples were cut to the dimensions (18 × 18 × 60) mm. The hardening process was carried out in a Bosio EUPK 6/1200 electric laboratory furnace without a protective atmosphere followed by oil quenching. The samples were placed in the furnace at room temperature, heated to 650 °C in 1 h and held at 650 °C for 20 min, then heated to 850 °C in 30 min and held at 850 °C for 20 min, the final heating step to the quenching temperature was carried out in 45 min and the samples were held at the quenching temperature for 20 min, before quenching in oil. The quenching temperatures were (1030, 1060, 1080 and 1100) °C. The oil temperature was 60 °C. The samples were then tempered in a vacuum furnace under a vacuum at temperatures of (540, 580, 600, 620 and 640) °C with a holding time of 2.5 h. The samples were milled to remove 2 mm of the surface layer to avoid the influence of decarburization.

The metallographic samples were ground, polished and etched with Nital 5%. The microstructure was analysed with an Olympus DP70 light microscope and a Thermo Scientific Quattro S field-emission scanning electron microscope with energy-dispersive X-ray spectroscopy (EDS). Hardness values were measured on all the investigated samples using Vickers hardness method, HV10.

The commercial software Thermo-Calc version 2022b was used for the CALPHAD calculations. The Thermo-Calc Software TCFE10 Steels/Fe-alloys database was selected to obtain the thermodynamic data for the calculations. We used the Equilibrium Calculator and selected the Property Diagram calculation type, from

which we obtained diagrams showing the amount of thermodynamically stable phases in the samples studied.

3 RESULTS AND DISCUSSION

3.1. CALPHAD calculations

The CALPHAD calculations (**Figures 1–4**) show the amount of thermodynamically stable phases in the analysed samples in the temperature range between 500 and 1300 °C. **Table 2** also lists all transformation and precipitation temperatures for all the investigated samples. In the reference sample 0 (**Figure 1**), the M6C ((Mo, Fe, W)$_6$C) carbides start to precipitate first at 1087 °C, followed by MC (WC) carbides at 810 °C. At 858 °C we have the Ae$_3$ at which the transformation from austenite to ferrite begins. The transformation ends at 797 °C, i.e., at the A$_{e1}$ temperature.

In the sample Nb (**Figure 2**), the MC (NbC) carbides start to precipitate first at 1253 °C, followed by M6C ((Mo, Fe, W, Nb)$_6$C) carbides at 1096 °C and the last carbides to precipitate are also MC (WC) carbides at 809 °C. At 860 °C we have the A$_{e3}$ temperature at which the transformation from austenite to ferrite begins. The transformation ends at 797 °C, i.e., at the A$_{e1}$ temperature.

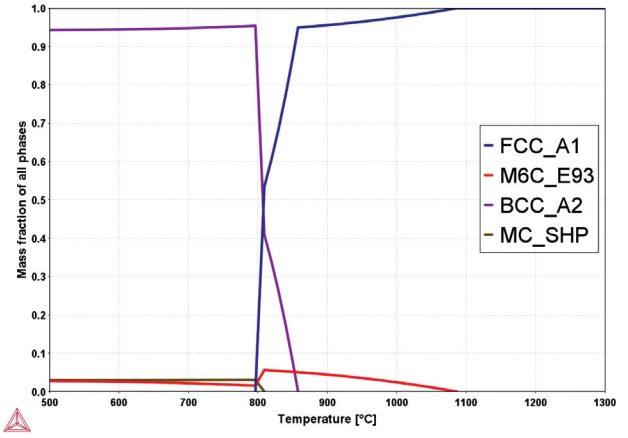

Figure 1: CALPHAD calculations of the equilibrium amount of phases in sample 0 between 500 °C and 1300 °C

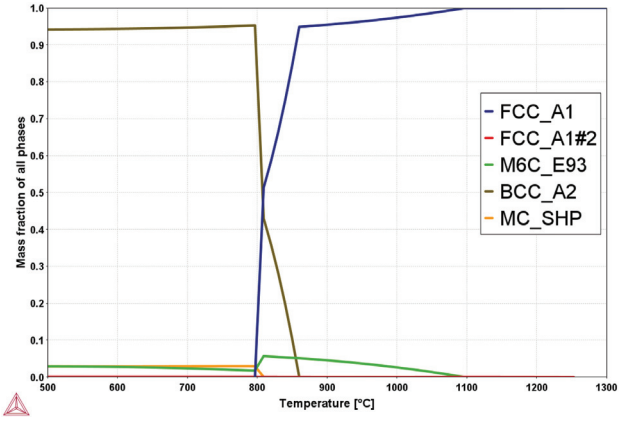

Figure 2: CALPHAD calculations of the equilibrium amount of phases in sample Nb between 500 °C and 1300 °C

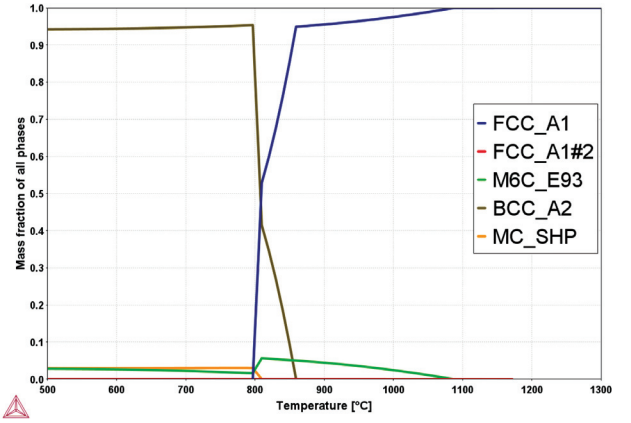

Figure 3: CALPHAD calculations of the equilibrium amount of phases in sample Ta between 500 and 1300 °C

In the Ta sample (**Figure 3**), the MC carbides (TaC) begin to precipitate first at 1172 °C, followed by the M6C carbides ((Mo, Fe, W, Ta)$_6$C) at 1087 °C and the MC carbides (WC), which precipitates last at 810 °C. At 859 °C, we have the A$_{e3}$ temperature at which the transformation from austenite to ferrite begins. The transformation ends at 797 °C, i.e., at the A$_{e1}$ temperature.

In the Ti sample (**Figure 4**), the M6C ((Mo, Fe, W, Ti)$_6$C) carbides start to precipitate first at 1087 °C, followed by MC (TiC) carbides at 1057 °C and the last carbides to precipitate are also MC (WC) carbides at 810 °C. At 859 °C, we have the A$_{e3}$ temperature at which the transformation from austenite to ferrite begins. The transformation ends at 797 °C, which corresponds to the A$_{e1}$ temperature.

Table 2 lists all the equilibrium phases that are stable in the analysed samples. The Thermo-Calc designations are given with the corresponding phase and precipitation or transformation temperatures. It is obvious that the addition of microalloying elements (Nb, Ta and Ti) has no

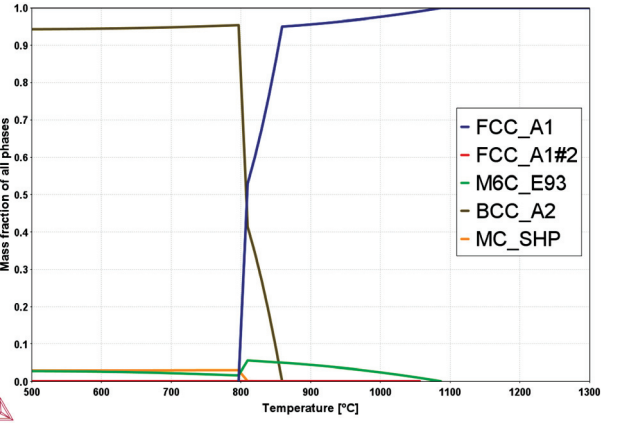

Figure 4: CALPHAD calculations of the equilibrium amount of phases in sample Ti between 500 °C and 1300 °C

influence on the transformation temperature between ferrite and austenite (A_{e3} and A_{e1}). It also has no influence on the precipitation temperature MC (WC), which is basically the same for all the samples analysed. There is a slight influence on the precipitation temperature of the M6C carbides, with the addition of Nb increasing the temperature by 9 °C. In the contrast, the addition of Ti and Ta has no effect on the precipitation temperature of the M6C carbides.[29,30] The main difference is the precipitation of additional carbides based on the microalloying elements. In the Nb sample, there is an additional precipitation of MC (NbC) carbides, which begins to precipitate at 1253 °C. The same applies to the Ta and Ti samples, where TaC carbides begin to precipitate at 1172 °C and TiC at 1057 °C.

Table 1: Precipitation temperatures for carbides and austenite – ferrite transformation temperatures (A_{e3} and A_{e1}) for all investigated samples in the temperature range between 500 and 1300 °C.

Sample	Thermo-Calc designation	Phase	Precipitation or transformation temperature (°C)
0	FCC_A1#2	/	/
	M6C_E93	$(Mo, Fe, W)_6C$	1087
	MC_SHP	WC	810
	BCC_A2	ferrite (α)	858 – A_{e3}
	FCC_A1	austenite (γ)	797 – A_{e1}
Nb	FCC_A1#2	NbC	1253
	M6C_E93	$(Mo, Fe, W, Nb)_6C$	1096
	MC_SHP	WC	809
	BCC_A2	ferrite (α)	860 – A_{e3}
	FCC_A1	austenite (γ)	797– A_{e1}
Ta	FCC_A1#2	TaC	1172
	M6C_E93	$(Mo, Fe, W, Ta)_6C$	1087
	MC_SHP	WC	810
	BCC_A2	ferrite (α)	859 – A_{e3}
	FCC_A1	austenite (γ)	797 – A_{e1}
Ti	M6C_E93	$(Mo, Fe, W, Ti)_6C$	1087
	FCC_A1#2	TiC	1057
	MC_SHP	WC	810
	BCC_A2	ferrite (α)	859 – A_{e3}
	FCC_A1	austenite (γ)	797 – A_{e1}

3.2. Quenching and tempering

Samples were quenched from austenitising temperatures of (1030, 1060, 1080 and 1100) °C. The austenitisation holding time was 25 min. The samples were then tempered for two hours at different temperatures (540, 580, 620 and 640) °C. Under all conditions, a bainitic-martensitic microstructure developed after quenching. Furthermore, all samples were free of primary carbide.

The hardness increases in most cases with increasing austenitisation temperature (**Figure 5**). At an austenitisation temperature of 1030 °C, the sample without added microalloying elements (0) reaches an average hardness value of 425 HV10. The addition of niobium (Nb) and tantalum (Ta) has no effect on the increase in hardness at the selected austenitisation temperature. The addition of titanium (Ti) also proved effective even at a lower temperature and caused an increase in the hardness of the steel after quenching to an average value of 446 HV10. The relatively low hardness after quenching is attributed to a relatively high amount of bainite in the microstructure.

Increasing the austenitisation temperature to 1060 °C did not increase the hardness of the sample without added microalloying elements (0) and it remained at 425 HV10. A greater effect on the hardness increase is observed in the case of niobium additions (Nb), where the hardness increases to an average value of 459 HV10. An even greater increase in hardness after quenching was obtained in the case of the sample alloyed with tantalum (Ta), where the hardness after quenching is 468 HV10. The addition of titanium (Ti) at an austenitisation temperature of 1060 °C had no significant effect on the increase in hardness.

At an austenitisation temperature of 1080 °C, the hardness of the sample without added microalloying elements (0), increases to 484 HV10. This increase is related to an increase in the concentration of carbon and dissolved alloying elements in the steel matrix. The trend of increasing hardness after quenching is also observed when the sample is alloyed with titanium (Ti). The hardness increases to 461 HV10. The addition of niobium (Nb) and tantalum (Ta) at the austenitisation temperature had no significant effect on the increase in hardness. This remains the same at the values obtained as at the lower austenitisation temperature of 1060 °C.

When the austenitisation temperature rises to 1100 °C, a smaller drop in hardness to 473 HV10 is observed in the unmodified sample (0). At the selected temperature, the addition of niobium (Nb) has the greatest effect on the increase in hardness, which after quenching is 502 HV10, which is also the highest hardness achieved. The addition of titanium (Ti) also increases the hardness to a value of 485 HV10. The addition of tanta-

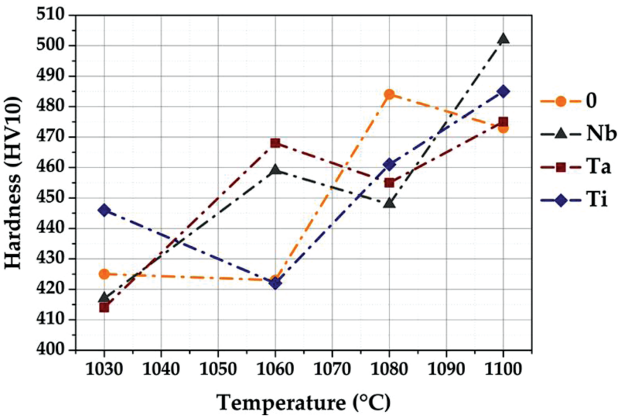

Figure 5: Hardness as a function of austenitisation temperature

lum (Ta) has the least effect on the increase of hardness among all the added alloying elements at the selected austenitisation temperature. The average hardness value is 475 HV10 and this is higher than the hardness of the reference sample (0).

The increase in the austenitisation temperature affected the increase in the size of the primary austenite crystal grains (**Figure 6**), especially of the reference sample (0) and the titanium-alloyed sample (Ti). Samples alloyed with niobium (Nb) and with tantalum (Ta) had a lesser effect on growth. At the highest austenitisation temperature of 1100 °C, all samples developed a coarse-grained microstructure. The hardness is most influenced by the change in the chemistry of the austenite matrix before quenching, the resulting bainite/martensite ration and the grain size.

The addition of niobium (Nb) and tantalum (Ta) had a large influence on the size of the crystal grains (**Figure 6**), which is also consistent with findings from literature sources.[26,29,30] Due to the small amount added, the addition of titanium (Ti) has been shown to be partially effective at lower austenitisation temperatures of up to 1060 °C, but has no major effect at higher temperatures. The austenitisation temperature range considered was between 1030 °C and 1100 °C. At the lowest austenitisation temperature selected, all the samples reach the same crystal grain size, i.e., about 30 µm, while the coarse grain size at 1100 °C was 90 µm, as shown in **Figure 7**. Increasing in the austenitisation temperature leads to the growth of the crystal grains, although there are large differences between the samples due to the influence of the additional alloying elements. In the case of sample (0) used as a reference, the more intensive growth of the crystal grains already begins at an austenitisation temperature of 1060 °C, at which the size increase more than doubles, i.e., from 30 µm to 65 µm. The effect of the titanium addition (Ti) has a lesser effect on inhibiting the growth of the crystal grains up to a temperature of 1060 °C, where the grains are 45 µm in size

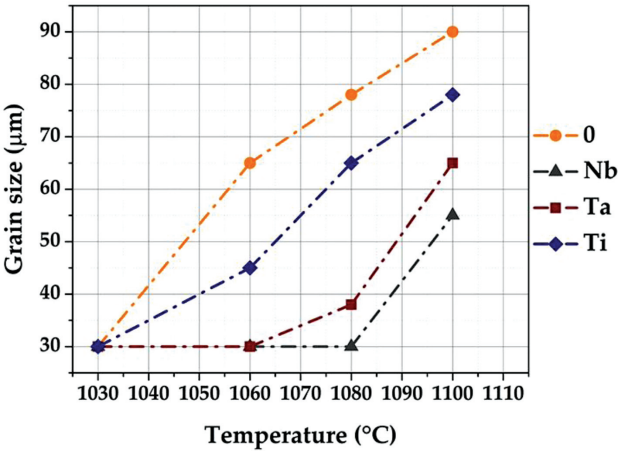

Figure 6: Grain size as a function of austenitisation temperature[5]

compared to the reference sample (0). As the austenitisation temperature increases, the effect of titanium on inhibiting the crystal growth decreases. The addition of tantalum (Ta) and niobium (Nb) successfully inhibits the growth of crystal grains up to a temperature of 1080°C, which remains unchanged in the case of niobium (Nb), i.e., 30 µm in size. Tantalum (Ta) also has a very similar effect to niobium (Nb), although the crystal grains in the Ta sample only partially grow to a size of 38 µm. The reason for the smaller crystal grain sizes is related to the formation of niobium- and tantalum-based precipitates or carbides, which precipitates at growth-inhibiting crystal grain boundaries. The addition of niobium proved to be most effective in inhibiting the crystal grain growth, even up to a temperature of 1100 °C. A more detailed discussion on the grain-growth mechanism in the samples is available in our previous work.[5]

The samples were hardened at austenitising temperatures of (1030, 1060, 1080 and 1100) °C and tempered at temperatures of (540, 580, 600, 620 and 640) °C, which are most commonly used to temper tools to the required hardness. As mentioned before, the tempering times

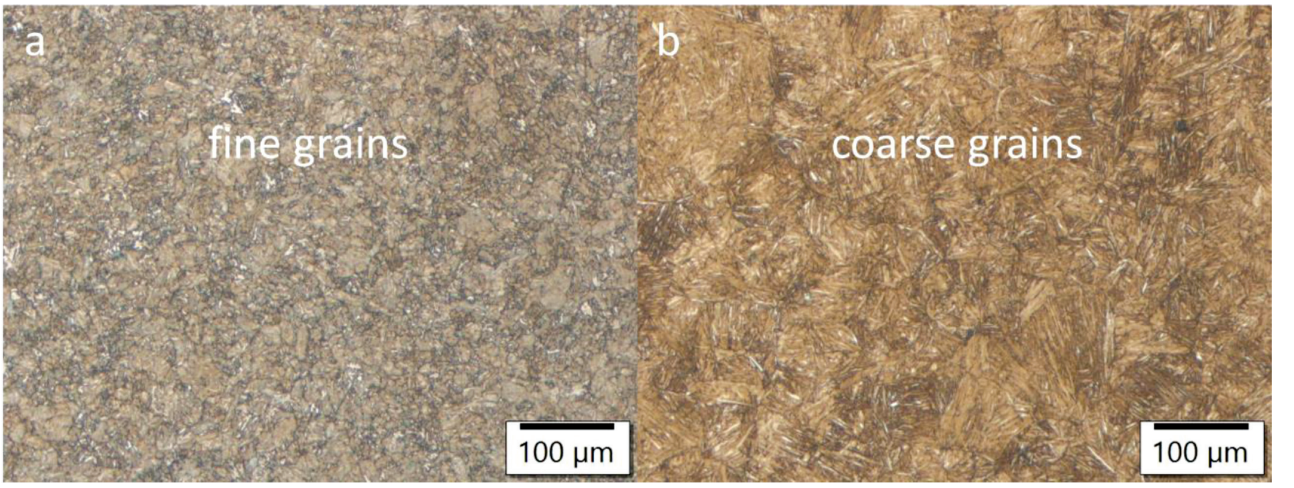

Figure 7: Representative microstructures of a) fine grain sample Nb – 1030 °C and b) coarse grain sample Ti – 1100 °C

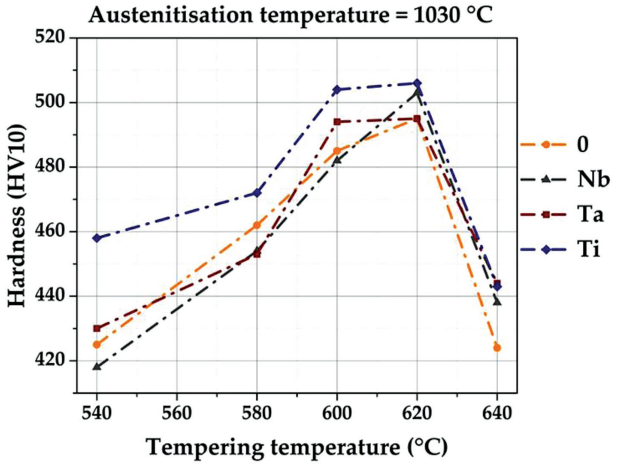

Figure 8: Tempering diagram for all the samples at austenitisation temperature of 1030 °C

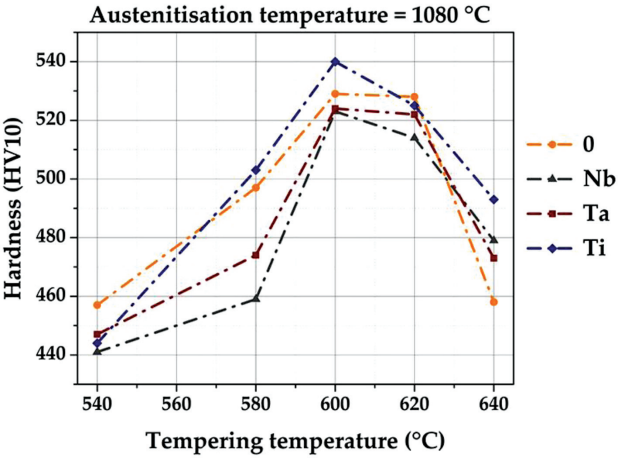

Figure 10: Tempering diagram for all the samples at austenitisation temperature of 1080 °C

were 2.5 h after reaching the temperature. With increasing tempering temperature, a secondary hardness peak was reached in all the samples. With increasing austenitisation temperature, the hardness after tempering and the value of the secondary peak hardness also increased. The highest secondary peak hardness values were achieved in the austenitisation temperature interval between 1080 °C and 1100 °C.

The alloying elements niobium, tantalum and titanium had an influence on the increase of the strength properties in the temperature range between (540 and 640) °C.

At an austenitisation temperature of 1030 °C (**Figure 8**), the Ti sample exhibits the maximum secondary peak hardness of 506 HV10. On the other hand, the Ta sample has the highest yield strength at 640 °C with a hardness value of 444 HV10. A predominantly bainitic microstructure with martensite was achieved by quenching from 1030 °C, as shown in **Figure 12a** and **12b**. The samples that were quenched from 1030 °C contained the most bainite of all the samples.

At the austenitisation temperature of 1060 °C (**Figure 9**), the maximum secondary peak hardness of the Nb sample is 533 HV10. Furthermore, this sample has the highest yield strength at 640 °C with a hardness value of 464 HV10. The microstructure contained both bainite and martensite; however, the bainite is still dominant (**Figure 12c** and **12d**).

At an austenitisation temperature of 1080 °C (**Figure 10**), the maximum secondary peak hardness of the Ti sample is 540 HV10. Furthermore, this sample has the highest yield strength at 640 °C with a hardness value of 493 HV10. The martensite content is higher than at 1030 °C or 1060 °C, but the sample still contains a fair amount of bainite (**Figure 12e** and **12f**).

At an austenitisation temperature of 1100 °C (**Figure 11**), the maximum secondary peak hardness of Nb and Ti samples is 542 HV. On the other hand, the Ta sample has the highest yield strength at 640 °C with a hardness value of 504 HV10. The bainite content is diminished, as the martensite becomes the dominant phase, as seen in **Figure 12g** and **12h**.

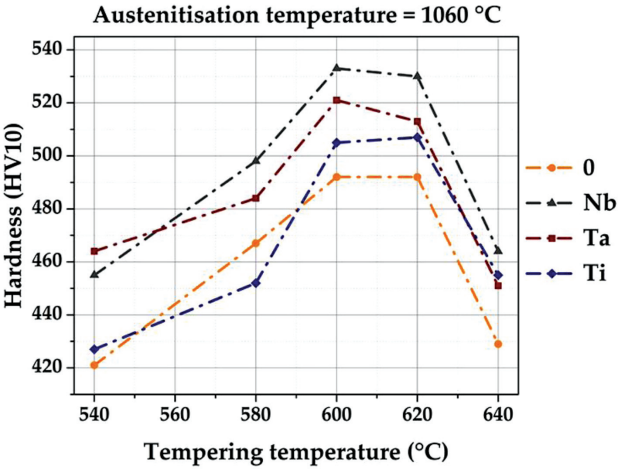

Figure 9: Tempering diagram for all the samples at austenitisation temperature of 1060 °C

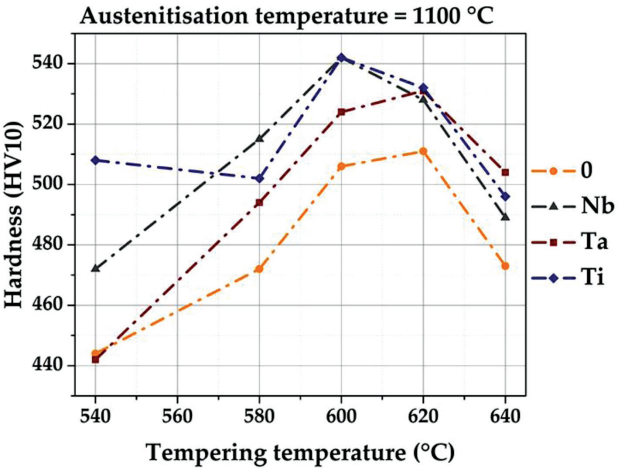

Figure 11: Tempering diagram for all the samples at austenitisation temperature of 1100 °C

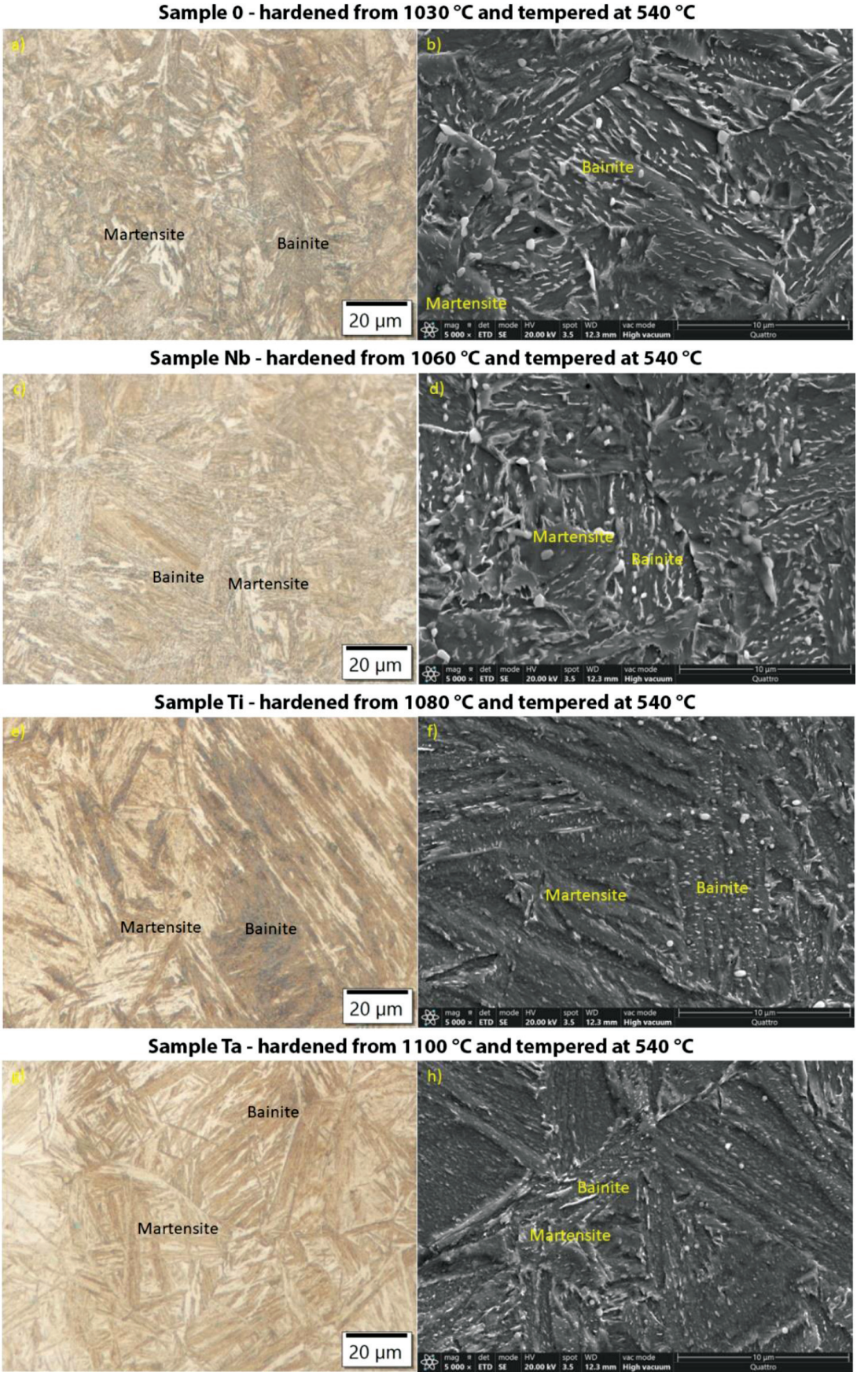

Figure 12: Microstructures of corresponding samples: a) and b) sample 0, c) and d) sample Nb, e) and f) sample Ti and g) and h) sample Ta

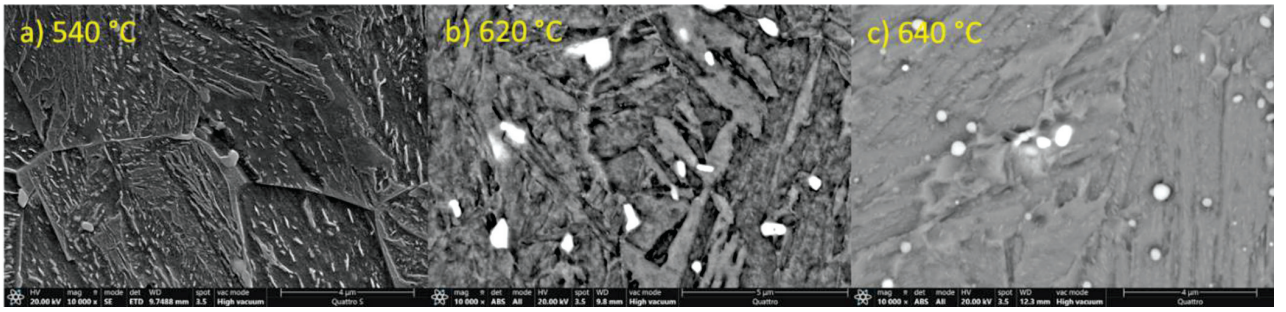

Figure 13: Coarsening of carbide microstructure of steel Ta hardened from 1100 °C, tempered at 540 °C

As the tempering temperatures rise the carbides coarsen and become rounder, as seen in **Figure 13**. Furthermore, tempering eliminates most of the needle-like carbides that form during quenching, mainly in the bainite and self-tempered martensite, as the carbon is combined with Mo-W carbides.[5] The changes in morphology are especially evident at 640 °C, where the typical round carbides, that have a very limited hardening ability, occur. These carbides are mostly found in tempered martensite.

4 CONCLUSIONS

The following conclusions can be drawn:

- Microalloying elements (Nb, Ta, and Ti) have a positive effect on grain-size retention during austenitisation and on the enhancement of hardness during tempering of Mo-W hot-work tool steel.
- CALPHAD calculations showed that the addition of microalloying elements influences the precipitation of additional carbides, depending on the element added (NbC, TaC, TiC).
- All samples exhibited a bainitic-martensitic microstructure after quenching and were free of primary carbides.
- The hardness increased in most cases with increasing austenitisation temperature.
- The addition of Nb and Ta showed the greatest effect on inhibiting the growth of austenite grains during austenitisation.
- The Ti addition had a limited effect on grain size refinement compared to Nb and Ta.
- Secondary hardening peaks were observed at tempering temperatures between 600 °C and 620 °C, and were more pronounced with microalloying.

5 REFERENCES

[1] A. Eser, C. Broeckmann, C. Simsir, Multiscale modeling of tempering of AISI H13 hot-work tool steel - Part 1: Prediction of microstructure evolution and coupling with mechanical properties, Comput. Mater. Sci., 113, (**2016**), 280–291, doi:10.1016/j.commatsci.2015.11.020

[2] J.Y. Li, Y. L. Chen, J. H. Huo, Mechanism of improvement on strength and toughness of H13 die steel by nitrogen, Mater. Sci. Eng. A, 640, (**2015**), 16–23, doi:10.1016/j.msea.2015.05.006

[3] R. Wu, W. Li, M. Chen, S. Huang, T. Hu, Improved mechanical properties by nanosize tungsten-molybdenum carbides in tungsten containing hot work die steels. Mater. Sci. Eng. A 812 (**2021**) 141140, doi:10.1016/j.msea.2021.141140

[4] R. Markežič, N. Mole, I. Naglič, R. Šturm, Time and temperature dependent softening of H11 hot-work tool steel and definition of an anisothermal tempering kinetic model. Mater. Today Commun. 22 (**2020**), doi:10.1016/j.mtcomm.2019.100744

[5] K. Grabnar, J. Burja, T. Balaško, A. Nagode, J. Medved, The influence of Nb, Ta and Ti modification on hot-work tool-steel grain growth during austenitization. Mater. Technol. 56 (**2022**) 331–338, doi:10.17222/mit.2022.486

[6] M. Vončina, T. Balaško, J. Medved, A. Nagode, Interface Reaction between Molten Al99.7 Aluminum Alloy and Various Tool Steels, Materials, 14 (**2021**) 24, 7708, doi:10.3390/ma14247708

[7] B. C. De Cooman, J. G. Speer, Fundamentals of Steel Product Physical Metallurgy; AIST, Association for Iron & Steel Techno-logy: Warrendale, PA, USA, 2011

[8] B. Podgornik, M. Sedlaček, B. Žužek, A. Guštin, Properties of tool steels and their importance when used in a coated system, Coatings, 10 (**2020**) 3, 265, doi:10.3390/coatings10030265

[9] Q. Zhou, X. Wu, N. Shi, J. Li, N. Min, Microstructure evolution and kinetic analysis of DM hot-work die steels during tempering. Mater. Sci. Eng. A, 528 (**2011**), 5696–5700, doi:10.1016/j.msea.2011.04.024

[10] A. Medvedeva, J. Bergström, S. Gunnarsson, J. Andersson, High-temperature properties and microstructural stability of hot-work tool steels. Mater. Sci. Eng. A, 523 (**2009**), 39–46, doi:10.1016/j.msea.2009.06.010

[11] N. B. Dhokey, S. S. Maske, P. Ghosh, Effect of tempering and cryogenic treatment on wear and mechanical properties of hot work tool steel (H13). Mater. Today Proc., 43 (**2021**), 3006–3013, DOI:10.1016/J.MATPR.2021.01.361

[12] E. Cabrol, C. Bellot, P. Lamesle, D. Delagnes, E. Povoden-Karadeniz, Experimental investigation and thermodynamic modeling of molybdenum and vanadium-containing carbide hardened iron-based alloys. J. Alloys Compd., 556 (**2013**), 203–209, doi:10.1016/j.jallcom.2012.12.119

[13] K. Chen, Z. Jiang, F. Liu, J. Yu, Y. Li, W. Gong, C. Chen, Effect of quenching and tempering temperature on microstructure and tensile properties of microalloyed ultra-high strength suspension spring steel. Mater. Sci. Eng. A, 766 (**2019**), doi:10.1016/j.msea.2019.138272

[14] G. Yang, X. Sun, Z. Li, X. Li, Q. Yong, Effects of vanadium on the microstructure and mechanical properties of a high strength low alloy martensite steel. Mater. Des., 50 (**2013**), 102–107, doi:10.1016/j.matdes.2013.03.019

[15] C. Zhang, Q. Wang, J. Ren, R. Li, M. Wang, F. Zhang, K. Sun, Effect of martensitic morphology on mechanical properties of an as-quenched and tempered 25CrMo48V steel. Mater. Sci. Eng. A, 534 (**2012**), 339–346, doi:10.1016/j.msea.2011.11.078

[16] C. Wang, M. Wang, J. Shi, W. Hui, H. Dong, Effect of microstructural refinement on the toughness of low carbon martensitic

steel. Scr. Mater., 58 (**2008**), 492–495, doi:10.1016/j.scriptamat.2007.10.053

[17] O. Haiko, V. Javaheri, K. Valtonen, A.; Kaijalainen, J. Hannula, J. Kömi, Effect of prior austenite grain size on the abrasive wear resistance of ultra-high strength martensitic steels. Wear, 454–455 (**2020**), 13–16, doi:10.1016/j.wear.2020.203336

[18] A. Karmakar, S. Kundu, S. Roy, S. Neogy, D. Srivastava, D. Chakrabarti, Effect of microalloying elements on austenite grain growth in Nb-Ti and Nb-V steels. Mater. Sci. Technol., 30 (**2014**), 653–664, doi:10.1179/1743284713Y.0000000386

[19] J. H. Hollomon, L. D. Jaffe, Time–temperature relations in tempering steels, Transactions of the American Institute of Mining and Metallurgical Engineers, 162 (**1945**), 223–249

[20] J. Mazurkiewicz, L. A. Dobrzański, E. Hajduczek, Comparison of the secondary hardness effect after tempering of the hot-work tool steels, Journal of Achievements in Materials and Manufacturing Engineering, 24 (**2007**), 119–122

[21] V. Leskovšek, B. Šuštaršič, G. Jutriša, The influence of austenitizing and tempering temperature on the hardness and fracture toughness of hot-worked H11 tool steel. J. Mater. Process. Technol., 178 (**2006**), 328–334, doi:10.1016/j.jmatprotec.2006.04.01

[22] H. Yang, J. H. Zhang, Y. Xu, M. A. Meyers, Microstructural characterization of the shear bands in Fe-Cr-Ni single crystal by EBSD. J. Mater. Sci. Technol., 24 (**2008**), 819–828

[23] J. Janovec, M. Svoboda, A. Výrostková, A. Kroupa, Time-temperature-precipitation diagrams of carbide evolution in low alloy steels. Mater. Sci. Eng. A, 402 (**2005**), 288–293, doi:10.1016/j.msea.2011.03.086

[24] J. G. Jung, J. S. Park, J. Kim, Y. K. Lee, Carbide precipitation kinetics in austenite of a Nb-Ti-V microalloyed steel. Mater. Sci. Eng. A, 528 (**2011**), 5529–5535

[25] J. Dong, X. Zhou, Y. Liu, C. Li, C. Liu, Q. Guo, Carbide precipitation in Nb-V-Ti microalloyed ultra-high strength steel during tempering. Mater. Sci. Eng. A, 683 (**2017**), 215–226, doi:10.1016/j.msea.2016.12.019

[26] J. Burja, A. Nagode, K. Grabnar, J. Medved, T. Balaško, Effect of Microalloying on Tempering of Mo-W High Thermal Conductivity Steel. Metallurgia Italiana, 114 (**2023**) 22–27

[27] E. Kaschnitz, P. Hofer, W. Funk, Thermophysical properties of a hot-work tool-steel with high thermal conductivity, Int. J. Thermophys., 34 (**2013**) 5, 843–850, doi:10.1007/s10765-012-1162-8

[28] I. Valls, A. Hamasaiid, A. Padré, High thermal conductivity and high wear resistance tool steels for cost-effective hot stamping tools, J. Phys. Conf. Ser., 896 (**2017**) 012046, doi:10.1088/1742-6596/896/1/012046

[29] J. Chen, C. Liu, Y. Liu, B. Yan, H. Li, Effects of tantalum content on the microstructure and mechanical properties of low-carbon RAFM steel. J. Nucl. Mater, 479 (**2016**), 295–301, doi.:10.1016/j.jnucmat.2016.07.029

[30] J. Foder, J. Burja, G. Klančnik, Grain size evolution and mechanical properties of Nb, V–Nb, and Ti–Nb boron type S1100QL steels. Metals, 11 (**2021**) 1–16, doi:10.3390/met11030492